J. Math. Biol. 44, 150–168 (2002)
Digital Object Identifier (DOI):
10.1007/s002850100116

Mathematical Biology

Mei-Hui Wang · Mark Kot · Michael G. Neubert

Integrodifference equations, Allee effects, and invasions

Received: 14 April 2000 / Revised version: 23 December 2000 /
Published online: 8 February 2002 –

Abstract. Models that describe the spread of invading organisms often assume no Allee effect. In contrast, abundant observational data provide evidence for Allee effects. We study an invasion model based on an integrodifference equation with an Allee effect. We derive a general result for the sign of the speed of invasion. We then examine a special, linear–constant, Allee function and introduce a numerical scheme that allows us to estimate the speed of traveling wave solutions.

1. Introduction

Ecologists are increasingly concerned with the effects of invading organisms (Mooney and Drake 1986; Drake et al. 1989; Hengeveld 1990; Shigesada and Kawasaki 1997; Ruiz et al. 2000). Thus, there is keen interest in models that can predict the rates of spread of invaders. Most invasion models have per capita growth rates that decrease with population density. For these models, one can determine the speed of invasion from a linearized version of the original model (van den Bosch et al. 1990; Mollison 1991). At the same time, many natural populations exhibit *Allee effects* (Allee 1938) or *depensation* (Clark 1990), showing an increase in per capita growth rate at low densities. This complicates matters: linearization may or may not give the correct speed of invasion if there is an Allee effect.

Allee effects may be weak or strong. Consider the density-dependent difference equation

$$N_{t+1} = f(N_t), \tag{1.1}$$

where N_t is the population size in generation t. We will assume that the mapping $f(N_t)$ satisfies

$$f(0) = 0, \quad f(1) = 1, \tag{1.2}$$

M.-H. Wang: Department of Mathematics, University of Tennessee, Knoxville, TN 37996-1300, USA. e-mail: meihui@math.utk.edu

M. Kot: Department of Applied Mathematics, Box 352420, University of Washington, Seattle, WA 98195-2420, USA. e-mail: kot@amath.washington.edu

M.G. Neubert: Biology Department, Woods Hole Oceanographic Institution, Woods Hole, MA 02543-1049, USA. e-mail: mneubert@whoi.edu

Key words or phrases: Integrodifference equations – Allee effects – Invasion models – Traveling waves

so that there is a trivial equilibrium at the origin and a nontrivial equilibrium that has been normalized to one. We will also assume that there is, at most, one other equilibrium between zero and one. Under these assumptions, the population exhibits an Allee effect if there exists a range of N_t in the interval [0, 1] such that

$$f(N_t) > f'(0)N_t. \tag{1.3}$$

(We use $'$ to denote an ordinary derivative.) This Allee effect is *strong* if

$$0 \leq f'(0) < 1; \tag{1.4}$$

it is *weak* if

$$f'(0) > 1. \tag{1.5}$$

A strong Allee effect introduces a population threshold. The population must surpass this threshold in order to grow. In contrast, a population with a weak Allee effect does not have a threshold. Many authors assume that all Allee effects are strong Allee effects. However, it is clear, from his examples, that Allee considered both strong and weak effects (Wang and Kot 2001). Figure 1 shows representative mappings with strong and weak Allee effects.

Allee effects can arise from a shortage of mates (Hopf and Hopf 1985; Hopper and Roush 1993; Veit and Lewis 1996; McCarthy 1997; Kuussaari et al. 1998), lack of effective pollination (Kunin 1993; Groom 1998), population fragmentation (Lamont et al. 1993; Gruntfest et al. 1997), or many other causes. Allee effects can slow down or stall an invasion (Lewis and Kareiva 1993; Lewis and van den Driessche 1993).

In this paper, we will analyze integrodifference equations (IDEs) with Allee effects. IDEs are models for populations with discrete generations and well-defined

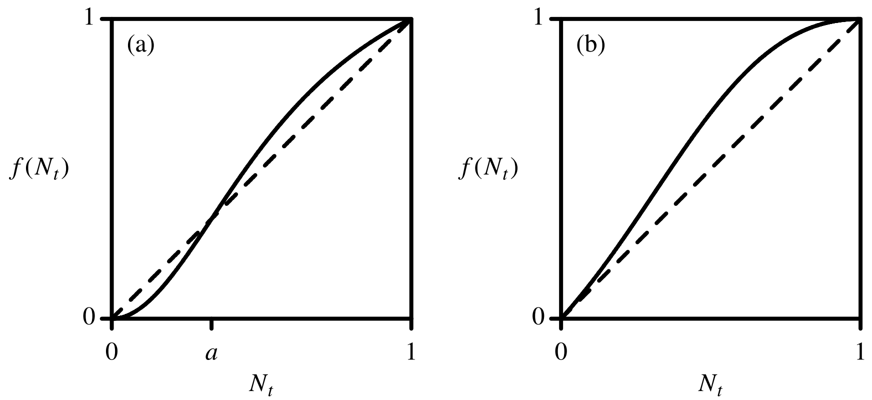

Fig. 1. Representative strong and weak Allee functions. The strong Allee function in subfigure (a) has population threshold a and satisfies the conditions that $f(N_t) > f'(0)N_t$, $0 \leq f'(0) < 1$, for a range of N_t in [0, 1]. The weak Allee function in subfigure (b) has no population threshold, but there is a range of N_t in [0, 1] such that $f(N_t) > f'(0)N_t$ with $f'(0) > 1$.

growth and dispersal stages. In the simplest case,

$$N_{t+1}(x) = \int_{-\infty}^{+\infty} k(x-y) f(N_t(y))\, dy, \tag{1.6}$$

where $N_t(x)$ is the population density at time t. Time is discrete; space is continuous. The function $f(N_t(x))$ describes the growth of the population during its sedentary stage. The redistribution kernel $k(x-y)$ is the probability density function for dispersal from a source at y. Neubert et al. (1995) describe how dispersal kernels can be derived from mechanistic models of dispersal. The integral tallies dispersal from all sources y.

Interest in IDEs in ecology has been increasing (Kot and Schaffer 1986; Hardin et al. 1988a, 1988b, 1990; Kot 1989, 1992; Andersen 1991; Hastings and Higgins 1994; Neubert et al. 1995; Allen et al. 1996; Kot et al. 1996; Veit and Lewis 1996; Brewster and Allen 1997; Brewster et al. 1997; Hart and Gardner 1997; Van Kirk and Lewis 1997; Latore et al. 1998; Clark 1998; Neubert and Caswell 2000; Neubert et al. 2000). One reason is that IDEs can handle an extremely wide variety of dispersal distributions. IDEs can have traveling wave solutions (Weinberger 1978, 1982; Lui 1982a, 1982b, 1983; Kot 1992; Hart and Gardner 1997) similar to those of reaction-diffusion equations. However, they can also give rise to accelerating invasions (Kot et al. 1996; Clark 1998).

Despite this interest, there has been little work on Allee effects and IDEs. Lewis and Veit (1996) used an IDE with an Allee effect to describe the dynamics of the House Finch invasion in eastern North America. Their model was quite general, but they relied on numerical simulations. In contrast, Kot et al. (1996) took an analytic approach, but focused on an extremely narrow limiting case. In this paper, we extend the work of Kot et al. (1996). We also hope to complement recent work on Allee effects in reaction-diffusion models (Lewis and Kareiva 1993; Cruickshank et al. 1999; Wang and Kot 2001).

In section 2, we derive a general result on the sign of the speed of invasion in the presence of an Allee effect. We follow this, in section 3, with an iterative scheme for estimating the rate of spread for a linear–constant Allee function. We use this scheme to estimate the rates of spread for both thin and fat-tailed dispersal kernels. We discuss the implications of our results in section 4.

2. A general result

In this section, we derive conditions that determine whether a traveling wave solution advances or retreats. We assume that the dynamics of a population are described by the IDE

$$N_{t+1}(x) = \int_{-\infty}^{+\infty} k(x-y) f(N_t(y))\, dy, \tag{2.1}$$

where the kernel $k(x-y)$ is a bounded and symmetric probability density function that satisfies

$$\int_{-\infty}^{+\infty} k(z)\, dz = 1. \tag{2.2}$$

We also assume that the recruitment f is an infinitely smooth function of N in the interval [0, 1] ($f \in C^{\infty}[0,1]$), that it increases with density,

$$f'(N) > 0, \tag{2.3}$$

and that it satisfies

$$f(N) \geq 0, \quad f(0) = 0, \quad f(1) = 1. \tag{2.4}$$

We are thus ignoring the possibility of overcompensation. Since f is strictly increasing, we can define its inverse f^{-1}.

Under these assumptions, it is reasonable to look for traveling wave solutions

$$N_{t+1}(x) = N_t(x - c) \tag{2.5}$$

that satisfy

$$\lim_{x \to -\infty} N_t(x) = 1, \quad \lim_{x \to +\infty} N_t(x) = 0 \tag{2.6}$$

(Weinberger 1978, 1982; Lui 1982a, 1982b, 1983; Kot 1992). The number c is the speed of the wave. If $c > 0$, the wave front moves toward low densities and the population always approaches the carrying capacity; the invader is successful. On the other hand, if $c < 0$, the wave front moves toward high densities and the population eventually goes extinct everywhere.

The traveling waves satisfy

$$N(x - c) = \int_{-\infty}^{+\infty} k(x - y) f(N(y))\, dy, \tag{2.7}$$

where we have now taken the liberty of dropping the subscripts on the N_t's. We will assume that these waves are infinitely smooth, $N(x) \in C^{\infty}$, and strictly decreasing, $N'(x) < 0$. We will also assume that

$$\lim_{x \to -\infty} \frac{d^i N}{dx^i} = \lim_{x \to +\infty} \frac{d^i N}{dx^i} = 0, \quad i = 1, 2, \ldots \tag{2.8}$$

and that there exists a positive number M such that

$$\left| \frac{d^i f(N(x))}{dx^i} \right| \leq M \text{ for all } x \text{ and } i = 1, 2, \ldots. \tag{2.9}$$

The condition that M is a uniform bound is important for the proof of Theorem 2.1. Lui (1983) discusses conditions that guarantee the existence of traveling waves for models with Allee effects.

Based on the above assumptions, we derive the following result:

Theorem 2.1. *For the traveling wave solutions of IDE (2.1),*

$$c < 0 \Longleftrightarrow \int_0^1 [f(N) - N]\, dN < 0, \tag{2.10}$$

$$c > 0 \Longleftrightarrow \int_0^1 [f(N) - N]\, dN > 0, \tag{2.11}$$

and

$$c = 0 \iff \int_0^1 [f(N) - N]\, dN = 0. \tag{2.12}$$

Here, $\iff$ *means "if and only if".*

Proof. If we subtract $N(x)$ from both sides of traveling-wave equation (2.7) and let $z \equiv x - y$, we obtain

$$N(x-c) - N(x) = \int_{-\infty}^{+\infty} k(x-y) f(N(y))\, dy - N(x) \tag{2.13}$$

$$= \int_{-\infty}^{+\infty} k(z) f(N(x-z))\, dz - N(x). \tag{2.14}$$

Let us write $f(N(x-z))$ as the sum of an odd and an even function in z,

$$f(N(x-z)) = f_o(x,z) + f_e(x,z), \tag{2.15}$$

where

$$f_o(x,z) = \frac{1}{2}[f(N(x-z)) - f(N(x+z))], \tag{2.16}$$

$$f_e(x,z) = \frac{1}{2}[f(N(x-z)) + f(N(x+z))]. \tag{2.17}$$

Since $f(N(x-z))$ and $f(N(x+z))$ are bounded by zero and one, and because the kernel integrates to one, equation (2.2), the integrals of $k(z)f(N(x-z))$, $k(z)f_o(x,z)$, and $k(z)f_e(x,z)$ with respect to z each exist and

$$\int_{-\infty}^{+\infty} k(z) f(N(x-z))\, dz = \int_{-\infty}^{+\infty} k(z) f_o(x,z)\, dz + \int_{-\infty}^{+\infty} k(z) f_e(x,z)\, dz. \tag{2.18}$$

The first integral on the right hand side of equation (2.18) equals zero because $k(z)f_o(x,z)$ is an odd function in z. It follows that

$$N(x-c) - N(x) = \int_{-\infty}^{+\infty} k(z) f_e(x,z)\, dz - N(x). \tag{2.19}$$

If we multiply equation (2.19) by $df(N(x))/dx$ and integrate with respect to x from $-\infty$ to $+\infty$, we get

$$\int_{-\infty}^{+\infty} [N(x-c) - N(x)] \frac{df}{dx}\, dx = \int_{-\infty}^{+\infty} \int_{-\infty}^{+\infty} k(z) f_e(x,z) \frac{df}{dx}\, dz\, dx - \int_{-\infty}^{+\infty} N(x) \frac{df}{dx}\, dx, \tag{2.20}$$

where

$$\frac{df}{dx} \equiv \frac{d}{dx}\, [f(N(x))]. \tag{2.21}$$

Since f is a strictly increasing function of N and N is a strictly decreasing function of x, the derivative of f with respect to x is negative. The integrand

$k(z) f_e(x, z) df/dx$ is thus of one sign. By Tonelli's theorem (Wheeden and Zygmund 1977), we can switch the order of integration in the first integral on the right hand side of equation (2.20).

Let us expand $f_e(x, z)$ as a Taylor series in z,

$$f_e(x, z) = f(N(x)) + \sum_{i=1}^{\infty} \frac{z^{2i}}{(2i)!} \frac{d^{2i}}{dx^{2i}} \; [f(N(x))]. \tag{2.22}$$

It follows that

$$\begin{aligned}\int_{-\infty}^{+\infty} [N(x-c) - N(x)] \frac{df}{dx} \, dx &= \int_{-\infty}^{+\infty} [f(N(x)) - N(x)] \frac{df}{dx} \, dx \\ &\quad + \int_{-\infty}^{+\infty} \int_{-\infty}^{+\infty} \sum_{i=1}^{\infty} J_i(x, z) \, dx \, dz, \end{aligned} \tag{2.23}$$

where

$$J_i(x, z) \equiv k(z) \frac{z^{2i}}{(2i)!} \frac{d^{2i} f}{dx^{2i}} \frac{df}{dx} \tag{2.24}$$

and

$$\frac{d^{2i} f}{dx^{2i}} \equiv \frac{d^{2i}}{dx^{2i}} \; [f(N(x))]. \tag{2.25}$$

We will now show that the second integral on the right hand side of equation (2.23) vanishes. The bound (2.9) guarantees that $\{J_i(x, z)\}$ is a sequence of integrable functions in x. Moreover, for fixed z,

$$\sum_{i=1}^{\infty} \int_{-\infty}^{+\infty} |J_i(x, z)| \, dx = \sum_{i=1}^{\infty} \int_{-\infty}^{+\infty} k(z) \frac{z^{2i}}{(2i)!} \left| \frac{d^{2i} f}{dx^{2i}} \right| \left| \frac{df}{dx} \right| dx \tag{2.26}$$

$$\leq \sum_{i=1}^{\infty} M k(z) \frac{z^{2i}}{(2i)!} \int_{-\infty}^{+\infty} \left| \frac{df}{dx} \right| dx \tag{2.27}$$

$$\leq M k(z) \sum_{i=1}^{\infty} \frac{z^{2i}}{(2i)!} \tag{2.28}$$

$$\leq M k(z) \; [\cosh(z) - 1] < \infty. \tag{2.29}$$

Thus, by the Levi theorem for series (Apostol 1975),

$$\int_{-\infty}^{+\infty} \int_{-\infty}^{+\infty} \sum_{i=1}^{\infty} J_i(x, z) \, dx \, dz = \int_{-\infty}^{+\infty} \sum_{i=1}^{\infty} \int_{-\infty}^{+\infty} J_i(x, z) \, dx \, dz \tag{2.30}$$

or

$$\int_{-\infty}^{+\infty} \int_{-\infty}^{+\infty} \sum_{i=1}^{\infty} J_i(x, z) \, dx \, dz = \int_{-\infty}^{+\infty} \sum_{i=1}^{\infty} k(z) \frac{z^{2i}}{(2i)!} S_i \, dz, \tag{2.31}$$

where

$$S_i \equiv \int_{-\infty}^{+\infty} \frac{d^{2i} f}{dx^{2i}} \frac{df}{dx} \, dx. \tag{2.32}$$

However, integration by parts shows that all of the S_i vanish:

$$S_1 = \int_{-\infty}^{+\infty} \frac{d^2 f}{dx^2}\frac{df}{dx}\,dx = \frac{1}{2}\left(\frac{df}{dx}\right)^2\Bigg|_{-\infty}^{+\infty} = \frac{1}{2}\left(\frac{df}{dN}\frac{dN}{dx}\right)^2\Bigg|_{-\infty}^{+\infty} = 0, \tag{2.33}$$

$$S_2 = \int_{-\infty}^{+\infty} \frac{d^4 f}{dx^4}\frac{df}{dx}\,dx = \left(\frac{d^3 f}{dx^3}\frac{df}{dx}\right)\Bigg|_{-\infty}^{+\infty} - \int_{-\infty}^{+\infty} \frac{d^3 f}{dx^3}\frac{d^2 f}{dx^2}\,dx \tag{2.34}$$

$$= 0 - \frac{1}{2}\left(\frac{d^2 f}{dx^2}\right)^2\Bigg|_{-\infty}^{+\infty} = 0, \tag{2.35}$$

and

$$S_i = \int_{-\infty}^{+\infty} \frac{d^{2i} f}{dx^{2i}}\frac{df}{dx}\,dx \tag{2.36}$$

$$= \left(\frac{d^{2i-1} f}{dx^{2i-1}}\frac{df}{dx}\right)\Bigg|_{-\infty}^{+\infty} - \int_{-\infty}^{+\infty} \frac{d^{2i-1} f}{dx^{2i-1}}\frac{d^2 f}{dx^2}\,dx \tag{2.37}$$

$$= \cdots\cdot = (-1)^{i-1}\int_{-\infty}^{+\infty} \frac{d^{i+1} f}{dx^{i+1}}\frac{d^i f}{dx^i}\,dx \tag{2.38}$$

$$= \frac{(-1)^{i-1}}{2}\left(\frac{d^i f}{dx^i}\right)^2\Bigg|_{-\infty}^{+\infty} = 0, \quad i \geq 3. \tag{2.39}$$

Notice that the above calculations require

$$\lim_{x\to-\infty}\frac{d^i f}{dx^i} = \lim_{x\to+\infty}\frac{d^i f}{dx^i} = 0, \quad i = 1, 2, \ldots, \tag{2.40}$$

which can be deduced from asymptotic boundary condition (2.8) and bound (2.9) using the chain rule.

Since the integrals in equation (2.31) equal zero, integral equation (2.23) reduces to

$$\int_{-\infty}^{+\infty} [N(x-c) - N(x)]\,\frac{df}{dx}\,dx = \int_{-\infty}^{+\infty} [f(N(x)) - N(x)]\,\frac{df}{dx}\,dx \tag{2.41}$$

or

$$\int_{-\infty}^{+\infty} [N(x-c) - N(x)]\,\frac{df}{dx}\,dx = \int_{1}^{0} [f(N) - N]\,df(N). \tag{2.42}$$

Setting $y \equiv f(N)$ gives us that

$$\int_{1}^{0} [f(N) - N]\,df(N) = -\int_{0}^{1} y\,dy + \int_{0}^{1} f^{-1}(y)\,dy. \tag{2.43}$$

Since the sum of the two areas bounded by

$$y = 1, \quad N = 0, \quad y = f(N) \tag{2.44}$$

and

$$y = 0, \quad N = 1, \quad y = f(N) \tag{2.45}$$

equals one, we have

$$\int_0^1 f^{-1}(y)\, dy = 1 - \int_0^1 f(N)\, dN. \tag{2.46}$$

It follows that

$$\int_{-\infty}^{+\infty} [N(x-c) - N(x)] \frac{df}{dx}\, dx = -\int_0^1 N\, dN + 1 - \int_0^1 f(N)\, dN \tag{2.47}$$

or

$$\int_{-\infty}^{+\infty} [N(x-c) - N(x)] \frac{df}{dx}\, dx = \int_0^1 [N - f(N)]\, dN. \tag{2.48}$$

Since N is a strictly decreasing function of x and the derivative of f with respect to x is negative, we have

$$c > 0 \Longleftrightarrow N(x-c) - N(x) > 0 \text{ on } (-\infty, \infty) \tag{2.49}$$

$$\Longleftrightarrow \int_{-\infty}^{+\infty} [N(x-c) - N(x)] \frac{df}{dx}\, dx < 0 \tag{2.50}$$

$$\Longleftrightarrow \int_0^1 [f(N) - N]\, dN > 0. \tag{2.51}$$

Similarly, we can show that result (2.10) for the negative sign of the speed and result (2.12) for the steady-state solution hold. □

Theorem 2.1 implies that the wave is advancing if and only if

$$\int_0^1 [f(N) - N]\, dN > 0 \tag{2.52}$$

and that it is retreating if and only if

$$\int_0^1 [f(N) - N]\, dN < 0. \tag{2.53}$$

The wave is a steady state if the area below the function f and above the 45° line equals the area above the function f and below the 45° line,

$$\int_0^1 [f(N) - N]\, dN = 0. \tag{2.54}$$

Example 2.1. *Consider IDE (2.1) with function*

$$f(N) = \frac{RN^2}{1 + (R-1)N^2}, \tag{2.55}$$

where $R > 2$. Under the assumptions at the beginning of this section, we can determine the sign of the speed c of the wave solution for various choices of R.

Since

$$\int_0^1 [f(N) - N]\, dN = \frac{R}{R-1}\left(1 - \frac{\tan^{-1}(\sqrt{R-1})}{\sqrt{R-1}}\right) - \frac{1}{2}, \tag{2.56}$$

we conclude that $c > 0$ if and only if

$$\frac{R}{R-1}\left(1 - \frac{\tan^{-1}(\sqrt{R-1})}{\sqrt{R-1}}\right) > \frac{1}{2} \tag{2.57}$$

or

$$R > 3.2952\ldots. \tag{2.58}$$

We also have $c < 0$ for $R < 3.2952\ldots$ and $c = 0$ for $R = 3.2952\ldots$. Figure 2 shows the function f and traveling wave solutions for $R = 5.0$, 3.2952, and $2.\bar{3}$. □

3. Estimating invasion speed: a numerical scheme

Theorem 2.1 determines the direction of a traveling wave solution of IDE (2.1) with an Allee effect. The theorem does not give us the actual speed. Unfortunately, even estimating the speed for most Allee functions is difficult. In this section, we develop a numerical scheme to estimate the invasion speed for a particularly simple growth function (Neubert 1997):

$$f(N_t) = \begin{cases} \lambda N_t, & N_t < a, \\ 1, & N_t > a, \end{cases} \tag{3.1a}$$

where

$$0 \le \lambda \le \frac{1}{a}, \quad 0 < a < 1 \tag{3.1b}$$

(see Figure 3).

Notice that $f(N_t)$ has a strong Allee effect if

$$0 \le \lambda < 1, \tag{3.2}$$

a weak Allee effect if

$$1 < \lambda < \frac{1}{a}, \tag{3.3}$$

and no Allee effect if

$$\lambda = \frac{1}{a}. \tag{3.4}$$

We study IDE (2.1) with a symmetric kernel and the linear–constant Allee function (3.1). We introduce a numerical scheme for estimating the speed of the traveling wave solutions.

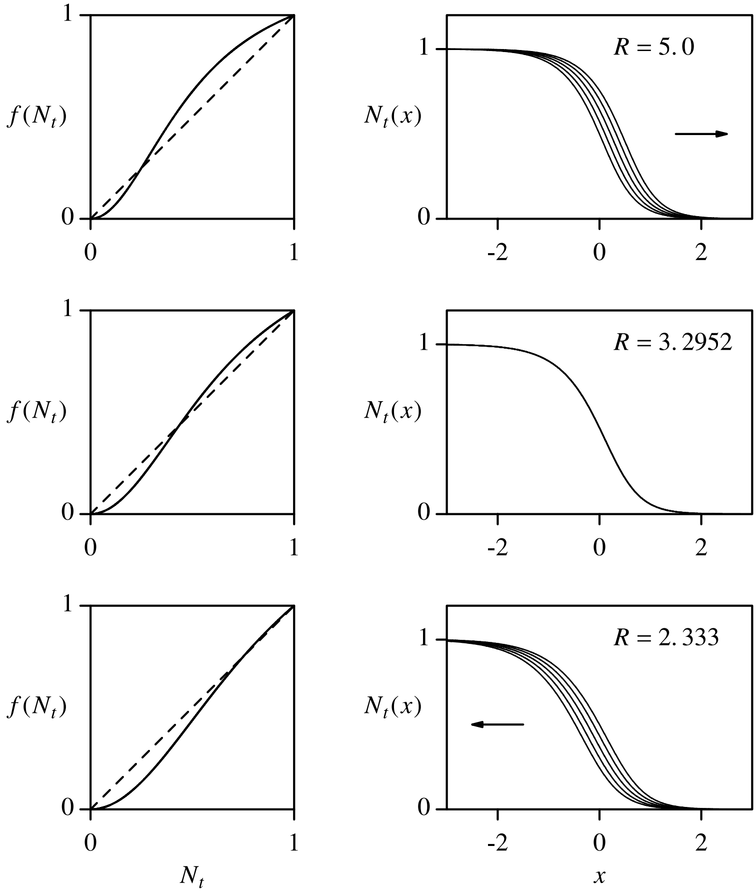

Fig. 2. A rational function and its traveling wave solutions for various choices of the parameter R. The function f, equation (2.55), is shown on the left for $R = 5$ (top), $R = 3.2952$ (middle), and $R = 7/3$ (bottom). The traveling wave solutions for these parameters are shown on the right. If the area between the function f and the 45° line is positive (top), the waves move to the right. If this area is negative (bottom), the waves move to the left. If this area is zero (middle), the traveling wave is a steady-state cline. The waves were simulated by integrating IDE (1.6) with 2^{13} mesh points and an FFT-assisted implementation of the trapezoidal rule. The kernel was the Laplace distribution, in Table 1, with $\alpha = 3$. Each panel shows five iterates of the traveling wave.

3.1. Traveling wave solutions

To estimate the speed of invasion, we look for a traveling wave solution. Suppose this traveling wave is moving to the right and that it attains the threshold value a at $x = 0$ and time t. Traveling-wave equation (2.7) and equation (3.1a) imply that the traveling wave satisfies

$$N(x - c) = \lambda \int_0^\infty k(x - y)N(y)dy + G(x), \tag{3.5a}$$

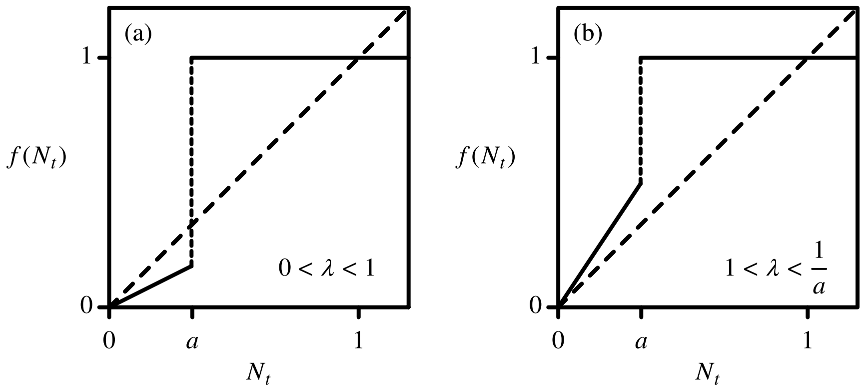

Fig. 3. The linear–constant Allee function. The function is defined by equations (3.1a) and (3.1b); it consists of a linear ramp of slope λ and a constant top. The function has (a) a strong Allee effect for $0 \leq \lambda < 1$ and (b) a weak Allee effect for $1 < \lambda < 1/a$. There is no Allee effect for $\lambda = 1/a$.

$$N(0) = a, \tag{3.5b}$$

where

$$G(x) \equiv 1 - \int_{-\infty}^{x} k(z)dz. \tag{3.5c}$$

We have, once again, dropped the subscript on N_t. Equation (3.5a) is a Wiener–Hopf equation (Gohberg and Fel'dman 1974). If $c = 0$, then equation (3.5a) is a one-sided or Wiener–Hopf integral equation of the second kind (Hochstadt 1973; Pipkin 1991).

For the case $\lambda = 0$, system (3.5) reduces to

$$N(x) = G(x + c), \tag{3.6a}$$

$$G(c) = a. \tag{3.6b}$$

We may thus conclude that the traveling wave solution takes the shape of the function $G(x)$ and that the speed c is given by equation (3.6b), or

$$c = G^{-1}(a) \tag{3.7}$$

(see Kot et al. 1996 for details).

For the case $\lambda \neq 0$, we will try to solve system (3.5) by considering a Neumann series (Pipkin 1991) of the form

$$N(x) = \sum_{i=0}^{\infty} \lambda^i u_i(x). \tag{3.8}$$

After substituting this series into system (3.5) and matching powers of λ, we obtain

$$u_0(x) = G(x + c), \tag{3.9a}$$

$$u_i(x) = \int_0^{\infty} k(x+c-y)u_{i-1}(y)\,dy, \qquad i = 1, 2, \ldots, \tag{3.9b}$$

$$a = G(c) + u_1(0)\lambda + u_2(0)\lambda^2 + \ldots. \tag{3.9c}$$

For Wiener–Hopf equations, numerical analysts commonly use a finite-section approximation (Atkinson 1969; Sloan and Spence 1986; Hoog and Sloan 1987; Anselone and Sloan 1988). This approximation allows us to replace the infinite upper limit of integration with an appropriate positive finite number L, so that iterative method (3.9) becomes

$$u_0(x) = G(x+c), \tag{3.10a}$$

$$u_i(x) = \int_0^{L} k(x+c-y)u_{i-1}(y)\,dy, \qquad i = 1, 2, \ldots, \tag{3.10b}$$

$$a = G(c) + u_1(0)\lambda + u_2(0)\lambda^2 + \ldots. \tag{3.10c}$$

The accuracy of this method is sensitive to the choice of L.

If we choose a value of c, we can iterate equation (3.10b) starting with the function $G(x+c)$. For the integration, we use a fast-Fourier-transform-assisted implementation of the trapezoidal rule (Andersen 1991). For each iteration, we evaluate $u_i(x)$ at the origin to get the next coefficient in equation (3.10c). Equation (3.10c) gives the relationship between the speed c and λ. Since all of the u_i are positive, Descartes's rule of signs guarantees that equation (3.10c) has a single positive root λ for fixed c. We determine this root and solve for λ as a function of c (or, equivalently, for c as a function of λ) numerically using Brent's method (Press et al. 1986).

To determine the speed c using straightforward numerical simulation, one must track a traveling wave as it crosses a large spatial domain. More convergence iterations means larger domains. Our new scheme allows us to compute additional terms in our series on a domain of fixed size, and to determine the effects of this size on the accuracy of our answers.

3.2. Numerical examples

We applied numerical method (3.5) to four different kernels (see Table 1). Two of these kernels, the normal distribution and the Laplace distribution, are "thin-tailed" distributions that have moment generating functions. The other two distributions, the exponential square root distribution and the Cauchy distribution, are "fat-tailed" kernels that do not have moment generating functions.

Figure 4 shows plots of speed c as a function of λ for these four kernels with $a = 0.5$. We know, from previous work (Kot et al. 1996), that fat-tailed kernels give rise to accelerating invasions and that strong Allee effects can turn accelerating invasions into constant-speed invasions. Figure 4 confirms these results. Our numerical results suggest that weak Allee effects may, on occasion, have the same effect. For the exponential square root distribution, there are weak Allee effects for

Table 1. Distributions $k(x)$ and corresponding functions $G(x)$.

Distribution	$k(x)$	$G(x)$
Laplace	$\frac{1}{2}\alpha e^{-\alpha\|x\|}$	$\frac{1}{2}e^{-\alpha x}$, if $x \geq 0$ $1-\frac{1}{2}e^{\alpha x}$, if $x < 0$
Normal	$\frac{1}{\sqrt{2\pi}\sigma}e^{-x^2/2\sigma^2}$	$\frac{1}{\sqrt{2\pi}\sigma}\int_x^\infty e^{-z^2/2\sigma^2}dz$ $=\frac{1}{2}\operatorname{erfc}\left(\frac{x}{\sqrt{2}\sigma}\right)$
Exponential square root	$\frac{\alpha^2}{4}e^{-\alpha\sqrt{\|x\|}}$	$\frac{1}{2}(1+\alpha\sqrt{x})e^{-\alpha\sqrt{x}}$
Cauchy	$\frac{1}{\pi}\frac{\alpha}{(\alpha^2+x^2)}$	$\frac{1}{2}-\frac{1}{\pi}\tan^{-1}\left(\frac{x}{\alpha}\right)$

which the speed c appears to be finite. The exact location of the transition from accelerating invasions to constant-speed invasions appears to be kernel-specific and may well depend on the exact spectral radius of the associated integral operator.

The curves for the thin-tailed normal kernel and Laplace distribution are concave up for strong Allee effects ($\lambda < 1$) and for some range of weak Allee effects, but concave down for large λ. An analysis of a related reaction-diffusion model (Wang and Kot 2001) suggests that each curve's inflection point marks the boundary between two domains: the speed of invasion is determined by linearization to the right but not to the left of the inflection point. For thin-tailed kernels, linearization at the origin gives the correct speed of invasion for sufficiently weak Allee effects. Linearization at the origin gives incorrect speeds for fat-tailed kernels with any Allee effect.

The Laplace distribution is simple enough that we have also been able to derive an exact analytic solution to system (3.5) for this kernel. Suppose c is the wave speed. The wave solution corresponding to the concave-up portion for the Laplace curve in Figure 4, with $x > -c$, is

$$N(x) = ae^{-\rho x}, \tag{3.11}$$

where ρ and c satisfy

$$\rho = \alpha(1-\lambda a), \quad e^{\rho c} = \frac{\alpha^2\lambda}{\alpha^2-\rho^2}. \tag{3.12}$$

Using equations (3.12), we can solve for c as a function of λ,

$$c = \frac{1}{\alpha(1-a\lambda)} \ln\left[\frac{\lambda}{1-(1-a\lambda)^2}\right] \tag{3.13}$$

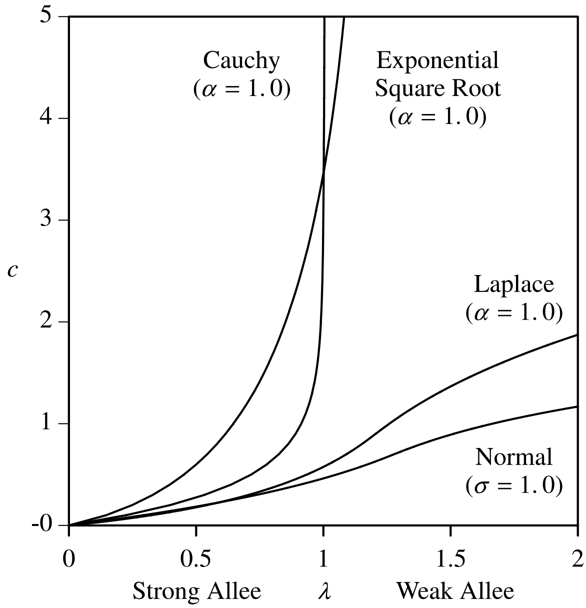

Fig. 4. The speed c as a function of λ for the Laplace ($\alpha = 1.0$), normal ($\sigma = 1.0$), exponential square root ($\alpha = 1.0$), and Cauchy ($\alpha = 1.0$) kernels and an Allee threshold of $a = 0.5$. The curves were computed using iterative scheme (3.5) with 2^{14} mesh points, order λ^{500}, and upper limits of integration of $L = 50$, $L = 30$, $L = 400$, and $L = 6000$. The thin-tailed Laplace and normal distributions generate finite-speed traveling waves for all positive λ. The speed diverges to infinity for the fat-tailed exponential square root distribution for some $\lambda > 1$ and for the fat-tailed Cauchy distributions at or near $\lambda = 1$.

The wave solution for the concave-down portion of the Laplace curve in Figure 4, with $x > -c$, is

$$N(x) = e^{-\delta x}(Ax + a), \tag{3.14}$$

where δ, c, and A satisfy

$$\lambda = \frac{\alpha^2 - \delta^2}{\alpha^2} \exp\left[\frac{2\delta^2}{\alpha^2 - \delta^2}\right], \quad c = \frac{2\delta}{\alpha^2 - \delta^2}, \tag{3.15}$$

and

$$A = -\frac{(\alpha - \delta)^2}{\lambda\alpha} - a(\delta - \alpha). \tag{3.16}$$

The wave solution on the interval $(-\infty, \; -c)$ is determined by the solution on the right-half real line ($x > 0$).

Speed formula (3.15) for the concave-down curve is the same as that derived by linearization (see Kot et al. 1996). The solid line in Figure 5 is the exact-speed curve obtained by plotting equations (3.13) and (3.15). Figure 5 also compares this exact solution with various orders of the numerical approximation. The agreement

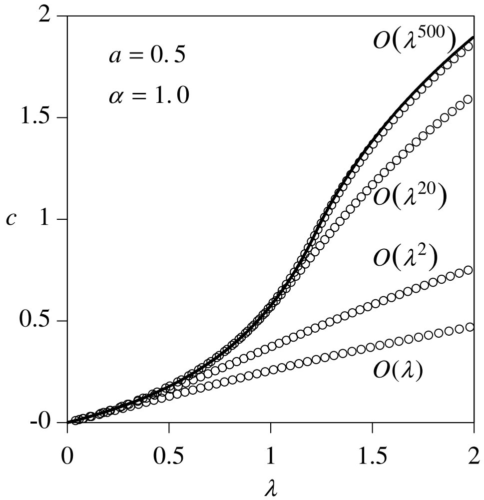

Fig. 5. The speed c as a function of λ for the Laplace distribution with $\alpha = 1$ and Allee threshold $a = 0.5$. The solid speed curve was obtaining analytically using equations (3.13) and (3.15). The speeds were also obtaining numerically, using iterative scheme (3.5). Integrations were performed using an FFT-assisted implementation of the trapezoidal rule with 2^{13} mesh points and an upper limit of integration of $L = 50$. The analytical curve and the order λ, order λ^2, order λ^{20}, and order λ^{500} numerical data are plotted.

is quite good for high order. To date, we have not been able to derive analytic solutions for the other kernels; we must instead rely on our numerical scheme. We hope to pursue general methods for solving system (3.5) in future work.

The choice of L is critical for our numerical results. If we choose an L too large, numerical instabilities arise. Conversely, if L is too small, we suffer a large error from neglecting too much of the integral. Consider the Cauchy distribution. When we fixed the speed c, the Allee threshold a, the order of the power series, and the number of mesh points n of integration, we obtained the effect of L on λ shown in Figure 6. For Figure 4, we chose L from the plateau between 4000 and 8000.

4. Discussion

Allee effects can slow down or reverse traveling wave solutions of reaction-diffusion equations (Lewis and Karieva 1993; Lewis and van den Driessche 1993). For integrodifference equations, Allee effects can play an additional role: they can turn accelerating invasions into constant-speed invasions (Kot et al. 1996). In this paper, we have tried to broaden our understanding of the effects of Allee effects on simple IDEs.

We have followed two complementary paths. In section 2, we have derived a simple formula for the sign of the speed of a traveling wave solution for a general, single-species IDE. This formula resembles a well-known result for the generalized Nagumo or bistable reaction-diffusion equation (Britton 1996; Keener and Sneyd 1998). Our result holds for redistribution kernels that are bounded and symmetric.

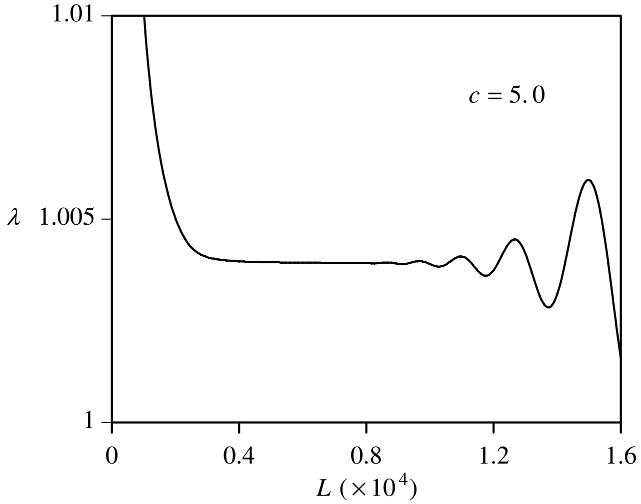

Fig. 6. The slope λ as a function of the upper limit of integration L for the Cauchy distribution. The plot shows the effect of the upper limit of integration on the value of λ produced using numerical scheme (3.5) for order 500 with 2^{14} mesh points, speed $c = 5.0$, and an Allee threshold of $a = 0.5$. As L increases, the slope λ approaches a plateau. For larger values of L, the slope oscillates due to a numerical instability. Care must be taken to choose a value of L from the plateau.

It suggests that the ultimate success of a sufficiently large invasion is independent of the exact redistribution kernel and depends only on the form of the function f. Loosely speaking, if the area of increase exceeds the area of decrease, à la equation (2.11), traveling waves will be waves of invasion.

While the exact form of a symmetric kernel does not have an obvious effect on the ultimate success of a sufficiently large invasion, it does have a profound influence on the speed with which that invasion occurs. In section 3, we developed a numerical scheme for estimating the speed of invasion for a linear–constant Allee function. This function shows all the important properties of more general Allee functions and can exhibit the full range of strong and weak Allee effects. By using this growth function, we have established an intimate link between traveling wave speeds for integrodifference equations with Allee effects and the theory of Wiener–Hopf equations.

We used our numerical scheme to estimate the speed of invasion for various thin-tailed and fat-tailed redistribution kernels in the presence of both strong and weak Allee effects. Thin-tailed kernels always gave rise to contant invasion speeds. For two fat-tailed examples, a strong Allee effect could always turn an accelerating invasion into a constant-speed invasion (or retreat). Based on our numerical results (Fig. 4), we conjecture that weak Allee effects can also convert accelerating invasions into constant speed-invasions. We expect that proving (or disproving) this conjecture will present significant mathematical challenges.

Most models with Allee effects have focused on a limited range of phenomena that involve thresholds. However, it is clear, from our own work and previous work by Hosono (1998), that weak Allee effects, with no threshold, may play the decisive role in analyses of speeds of invasion. Weak Allee effects are often subtle and pernicious. For example, Hosono showed that an inferior competitor can introduce a weak Allee effect into the growth function of a superior competitor. If this Allee effect is insufficiently weak, linearization at low densities will fail to give the correct speed of invasion (Hosono 1998, see also Wang and Kot 2001). We suspect, in light of our numerical results, that an inferior competitor can also turn the accelerating invasion of a superior competitor into a constant-speed invasion for some kernels, but not for others. We hope to determine if this is true in a future paper.

Acknowledgements. It is a pleasure to acknowledge Hal Caswell, Bill Fagan, Suzanne Lenhart, Mark Lewis, Pauline van den Driessche, and two anonymous reviewers for suggestions and/or discussions. We are grateful to the National Science Foundation (DMS-9973212) for their support.

References

Allee, W.C.: *The Social Life of Animals.* W. W. Norton and Co., New York 1938

Allen, E.J., Allen, L.J.S., Gilliam, X.: Dispersal and competition models for plants. *J. Math. Biol.* **34**, 445–481 (1996)

Andersen, M.: Properties of some density-dependent integrodifference-equation population models. *Math. Biosci.* **104**, 135–157 (1991)

Anselone, P.M., Sloan, I.H.: Numerical solutions of integral equations on the half line II: the Wiener–Hopf case. *J. Integ. Eqs. Appl.* **1,** 203–225 (1988)

Apostol, T.M.: *Mathematical Analysis.* Addition–Wesley Publishing Company, Inc. 1974

Atkinson, K.: The numerical solution of integral equations on the half-line. *SIAM J. Numer. Anal.* **6,** 375–397 (1969)

Brewster, C.C., Allen, J.C.: Spatiotemporal model for studying insect dynamics in large-scale cropping systems. *Environ. Entomol.* **26,** 473–482 (1997)

Brewster, C.C., Allen, J.C., Schuster, D.J., Stansly, P.A.: Simulating the dynamics of *Bemisia argentifoli* (Homoptera: Aleyrodidae) in an organic cropping system with a spatiotemporal model. *Environ. Entomol.* **26,** 603–616 (1997)

Britton, N.F.: *Reaction-Diffusion Equations and their Applications to Biology.* Academic Press, London 1986

Clark, C.W.: *Mathematical Bioeconomics: The Optimal Management of Renewable Resource.* John Wiley and Sons, New York 1990

Clark, J.S.: Why trees migrate so fast: confronting theory with dispersal biology and the paleorecord. *Am. Nat.* **152,** 204–224 (1998)

Cruickshank, I., Gurney, W.S.C., Veitch, A.R.: The characteristics of epidemics and invasions with thresholds. *Theor. Pop. Biol.* **56,** 279–292 (1999)

Drake, J.A., Mooney, H.A., di Castri, F., Groves, R.H., Kruger, F.J., Rejmanek, M., Williamson, M.: *Biological Invasions: A Global Perspective.* John Wiley and Sons, Chichester, UK 1989

Friedman, A.: *Foundations of Modern Analysis.* Holt, Rinehart, and Winston, Inc., New York 1970

Gohberg, I.C., Fel'dman, I.A.: *Convolution Equations and Projection methods for their solution.* American Mathematical Society, Providence, Rhode Island 1974

Gruntfest, Y., Arditi, R., Dombrovsky, Y.: A fragmented population in a varying environment. *J. Theor. Biol.* **185,** 539–547 (1997)
Groom, M.J.: Allee effects limit population viability of an annual plant. *Am. Nat.* **151,** 487–496 (1998)
Hardin, D.P., Takac, P., Webb, G.F.: A comparison of dispersal strategies for survival of spatially heterogeneous populations. *SIAM J. Appl. Math.* **48,** 1396–1423 (1988a)
Hardin, D.P., Takac, P., Webb, G.F.: Asymptotic properties of a continuous-space discrete-time population model in a random environment. *J. Math. Biol.* **26,** 361–374 (1988b)
Hardin, D.P., Takac, P., Webb, G.F.: Dispersion population models discrete in time and continuous in space. *J. Math. Biol.* **28,** 1–20 (1990)
Hart, D.R., Gardner, R.H.: A spatial model for the spread of invading organisms subject to competition. *J. Math. Biol.* **35,** 935–948 (1997)
Hastings, A., Higgins, K.: Persistence of transients in spatially structured ecological models. *Science* **263,** 1133–1136 (1994)
Hengeveld, R.: *Dynamics of Biological Invasions.* Chapman and Hall, London, UK 1990
Hochstadt, H.: *Integral Equations.* John Wiley and Sons, Inc. New York 1973
Hoog, F.D., Sloan I.H.: The finite-section approximation for integral equations on the half-line. *J. Austral. Math. Soc. Ser.* **B 28,** 415–434 (1987)
Hopf, F.A., Hopf, F.W.: The role of the Allee effect in species packing. *Theor. Pop. Biol.* **27,** 27–50 (1985)
Hopper K.R., Roush, R.T.: Mate finding, dispersal, number released, and the success of biological control introductions. *Ecol. Entomol.* **18,** 321–331 (1993)
Hosono, Y.: The minimal speed of traveling fronts for a diffusive Lotka–Volterra competition model. *Bull. Math. Biol.* **60,** 435–448 (1998)
Keener, J., Sneyd, J.: *Mathematical Physiology.* Springer-Verlag, New York 1998
Kot, M.: Diffusion-driven period-doubling bifurcations. *Biosystems* **22,** 279–287 (1989)
Kot, M.: Discrete-time traveling waves: ecological examples. *J. Math. Biol.* **30,** 413–436 (1992)
Kot, M., Schaffer, W.M.: Discrete-time growth-dispersal models. *Math. Biosci.* **80,** 109–136 (1986)
Kot, M., Lewis, M.A., van den Driessche, P.: Dispersal data and the spread of invading organisms. *Ecology* **77,** 2027–2042 (1996)
Kunin, W.E.: Sex and the single mustard: population density and pollinator behavior effects on seed-set. *Ecology* **74,** 2145–2160 (1993)
Kuussaari, M., Saccheri, I., Camara, M., Hanski, I.: Allee effect and population dynamics in the Glanville fritillary butterfly. *Oikos* **82,** 384–392 (1998)
Lamont, B.B., Klinkhamer, P.G.L., Witkowski, E.T.F.: Population fragmentation may reduce fertility to zero in *Banksia goodii* – a demonstration of the Allee effect. *Oecologia* **94,** 446–450 (1993)
Latore, J., Gould, P., Mortimer, A.M.: Spatial dynamics and critical patch size of annual plant populations. *J. Theor. Biol.* **190,** 277–285 (1998)
Lewis, M.A., Kareiva, P.: Allee dynamics and the spread of invading organisms. *Theor. Pop. Biol.* **43,** 141–158 (1993)
Lewis, M.A., van den Driessche, P.: Waves of extinction from sterile insect release. *Math. Biosci.* **116,** 221–247 (1993)
Lui, R.: A nonlinear integral operator arising from a model in population genetics, I. Monotone initial data. *SIAM J. Math. Anal.* **13,** 913–937 (1982a)
Lui, R.: A nonlinear integral operator arising from a model in population genetics, II. Initial data with compact support. *SIAM J. Math. Anal.* **13,** 938–953 (1982b)
Lui, R.: Existence and stability of traveling wave solutions of a nonlinear integral operator. *J. Math. Biol.* **16,** 199–220 (1983)

McCarthy, M.A.: The Allee effect, finding mates and theoretical models. *Ecol. Model.* **103,** 99–102 (1997)

Mollison, D.: Dependence of epidemics and population velocities on basic parameters. *Math. Biosc.* **107,** 255–287 (1991)

Mooney, H.A., Drake, J.A.: *Ecology of Biological Invasions of North America and Hawaii.* Springer-Verlag, New York (1986)

Neubert, M.G., Kot, M., Lewis, M.A.: Dispersal and pattern formation in a discrete-time predator-prey model. *Theor. Pop. Biol.* **48,** 7–43 (1995)

Neubert, M.G.: A simple population model with qualitatively uncertain dynamics. *J. Theor. Biol.* **189,** 399–411 (1997)

Neubert, M.G., Kot, M., Lewis, M.A.: Invasion speeds in fluctuating environments. *Proc. R. Soc. Lond. B* **267,** 1603–1610 and **267,** 2568–2569 (2000)

Neubert, M.G., Caswell, H.: Dispersal and demography: calculation and sensitivity analysis of invasion speeds for stage-structured populations. *Ecology.* **81,** 1613–1628 (2000)

Pipkin, A.C.: *A Course on Integral Equations.* Springer-Verlag, New York 1991

Press, W.H., Flannery B.P., Teukolsky, S.A., Vetterling, W.T.: *Numerical recipes: The Art of Scientific Computing.* Cambridge University Press, Cambridge 1986

Ruiz, G.M., Fofonoff, P.W., Carlton, J.T., Wonham, M.J., Hines, A.H.: Invasion of coastal marine communities in north America: apparent patterns, processes, and biases. *Annu. Rev. Ecol. Syst.* **31,** 481–531 (2000)

Shigesada, N., Kawasaki, K.: *Biological Invasions: Theory and Practice.* Oxford University Press, Oxford, UK 1997

Sloan, I.H., Spence, A.: Integral Equations on the half-line: a modified finite-section approximation. *Math. Comp.* **47,** 589–595 (1986)

van den Bosch, F., Metz, J.A.J., Diekmann, O.: The velocity of population spatial expansion. *J. Math. Biol.* **28,** 529–565 (1990)

Van Kirk, R.W., Lewis, M.A.: Integrodifference models for persistence in fragmented habitats. *Bull. Math. Biol.* **59,** 107–138 (1997)

Veit, R.R., Lewis, M.A.: Dispersal, population growth, and the Allee effect, Dynamics of the House Finch invasion of eastern North America. *Am. Nat.* **148,** 255–274 (1996)

Wang, M.H., Kot, M.: Speeds of invasion in a model with strong or weak Allee effects. *Math. Biosci.* **173,** 83–97 (2001)

Weinberger, H.F.: Asymptotic behavior of a model of population genetics. In, Chadam, J. (ed.), *Nonlinear Partial Differential Equations and Applications.* Lecture Notes in Mathematics **648,** 47–98 (1978)

Weinberger, H.F.: Long-time behavior of a class of biological models. *SIAM J. Math. Anal.* **13,** 353–396 (1982)

Wheeden, R.L., Zygmund, A.: *Measure and Integral: An Introduction to Real Analysis.* Marcel Dekker, Inc. New York 1977